Aging Cell (2007) **6**, pp139–153 Doi: 10.1111/j.1474-9726.2007.00270.x

Primary laminopathy fibroblasts display altered genome organization and apoptosis

Karen J. Meaburn,[1]* Erik Cabuy,[3] Gisele Bonne,[4] Nicolas Levy,[5] Glenn E. Morris,[6] Giuseppe Novelli,[7] Ian R. Kill[2] and Joanna M. Bridger[1]

[1]Laboratory of Nuclear and Genomic Health, [2]Cellular Gerontology Laboratory, Centre for Cell and Chromosome Biology, [3]Institute of Cancer Genetics and Pharmacogenomics, Division of Biosciences, School of Health Sciences and Social Care, Brunel University, Uxbridge, Middlesex, UB8 3PH, UK
[4]Inserm U582, Paris, France, Universite Pierre et Marie Curie-Paris 6, Faculté de Médecine, Paris, France, AP-HP, Groupe Hospitalier Pitié-Salpêtrière, U.F. Myogénétique et Cardiogénétique, service de Biochimie B, Paris, France
[5]Inserm U491, Génétique Médicale et Développement, Faculté de Médecine, 13385 Marseille Cedex 05, France
[6]Centre for Inherited Neuromuscular Disease, RJAH Orthopaedic Hospital, Oswestry, SY10 7AG, UK
[7]Department of Biopathology and Diagnostic Imaging, University of Rome Tor Vergata, Rome, Italy

Summary

A number of diseases associated with specific tissue degeneration and premature aging have mutations in the nuclear envelope proteins A-type lamins or emerin. Those diseases with A-type lamin mutation are inclusively termed laminopathies. Due to various hypothetical roles of nuclear envelope proteins in genome function we investigated whether alterations to normal genomic behaviour are apparent in cells with mutations in A-type lamins and emerin. Even though the distributions of these proteins in proliferating laminopathy fibroblasts appear normal, there is abnormal nuclear positioning of both chromosome 18 and 13 territories, from the nuclear periphery to the interior. This genomic organization mimics that found in normal nonproliferating quiescent or senescent cells. This finding is supported by distributions of modified pRb in the laminopathy cells. All laminopathy cell lines tested and an X-linked Emery–Dreifuss muscular dystrophy cell line also demonstrate increased incidences of apoptosis. The most extreme cases of apoptosis occur in cells derived from diseases with mutations in the tail region of the *LMNA* gene, such as Dunningan-type familial partial lipodystrophy and mandibuloacral dysplasia, and this correlates with a significant level of micronucleation in these cells.

Key words: apoptosis; A-type lamins; genome organization; laminopathies; micronucleation; nuclear architecture; quiescence, senescence.

Introduction

The cell nucleus is a highly organized organelle that houses the cell's genome. There are a number of nuclear structures involved in regulating the function of the cell nucleus (Foster & Bridger, 2005). One of these is the nuclear lamina located at the inner nuclear envelope, which contains and is associated with a number of proteins that interact with each other and the genome (Margalit *et al*., 2005a). Two of these proteins are the inner nuclear envelope type V intermediate filament proteins, the A-type lamins (lamin A and lamin C) encoded by the *LMNA* gene, and the integral membrane protein emerin encoded by the *EMD* gene. Both these proteins have DNA- and chromatin-binding abilities (Taniura *et al*., 1995; Stierle *et al*., 2003; Bengtsson & Wilson, 2004) and are therefore candidates for regulating genome function (Bridger & Bickmore, 1998; Foster & Bridger, 2005). A-type lamins and emerin are also binding partners of each other and so may elicit a cellular function in combination (Zastrow *et al*., 2004). Further, the A-type lamins have other roles in regulation of genomic function such as DNA replication (Spann *et al*., 1997 and references therein), proliferative cell cycle progression (Margalit *et al*., 2005a), transcription (Wilson, 2000; Lammerding *et al*., 2004) and most recently, aging (Bridger & Kill, 2004; Broers *et al*., 2006; Kudlow & Kennedy, 2006; Scaffidi & Misteli, 2006). Emerin may also be involved in the control of gene expression (Tsukahara *et al*., 2002) and chromatin organization (Margalit *et al*., 2005b). It is interesting that the A-type lamins are not only found at the nuclear periphery but also in foci deep within nuclei (Goldman *et al*., 1992; Bridger *et al*., 1993) associated with lamina-associated polypeptide 2 alpha (LAP2α) (Dechat *et al*., 2000) and retinoblastoma protein (pRb) (Markiewicz *et al*., 2002; Johnson *et al*., 2004). Emerin is also found at internal sites within nuclei, colocalized with A-type lamins (Manilal *et al*., 1998). Therefore, emerin is probably also a member of the complex containing pRb and LAP2α. Indeed, in two recent studies mutations in either *LMNA*

Correspondence
Joanna Bridger, Laboratory of Nuclear and Genomic Health, Centre for Cell and Chromosome Biology, Division of Biosciences, School of Health Sciences and Social Care, Brunel University, Uxbridge, Middlesex, UB8 3PH, UK.
Tel.: ++44-1895-266272; fax: ++44-1895-274348;
e-mail: joanna.bridger@brunel.ac.uk
**Present address: National Cancer Institute, National Institute of Health, 9000 Rockville Pike, Bethesda, MD 20892, USA.*

Accepted for publication *16 November 2006*

or *EMD* has been shown to lead to disruption of Rb-modulated pathways (Bakay *et al*., 2006; Melcon *et al*., 2006).

In the past decade a number of diseases have been attributed to mutations in both the *LMNA* gene (collectively termed laminopathies) and the *EMD* gene. *LMNA* related laminopathies include muscular dystrophies, dilated cardiomyopathies, type 2 diabetes, Charcot-Marie-Tooth type 2 B1 (CMT2B1), mandibuloacral dysplasia (MADA) lipodystrophy, and premature aging syndromes (for detail see Gruenbaum *et al*., 2005; Somech *et al*., 2005). Emerin gene mutations have so far led to X-linked Emery–Dreifuss muscular dystrophy (X-EDMD) (Bione *et al*., 1994). These diseases affect a wide range of tissue types including striated skeletal and cardiac muscle, nervous tissue, skin, adipose, tendon and bone. All the affected tissues are derived from mesenchymal stem cells and this appears to be a potential connection between the different diseases (Hutchison & Worman, 2004; Gotzmann & Foisner, 2005).

Studies on cells derived from Hutchinson-Gilford progeria syndrome (HGPS) patients have revealed the fraction of tissue culture cells displaying nuclear abnormalities increased with passage number (Bridger & Kill, 2004; Goldman *et al*., 2004; McClintock *et al*., 2006). Further, cells from patients with HGPS also display genomic instability (Liu *et al*., 2005), are hyperproliferative and have foreshortened lifespans in culture (Bridger & Kill, 2004) and towards the end of this lifespan in culture, they display an increased fraction of cells undergoing apoptosis (Bridger & Kill, 2004). Taken together, these data have led to the hypothesis that HGPS symptoms are due to tissues becoming senescent prematurely with a coincidental loss of cells that could lead to tissue degeneration *in vivo* (Stehbens *et al*., 1999). Others have demonstrated apoptosis associated with altered lamin A expression, i.e. in spermatocytes of *Lmna* knock-out mice (Alsheimer *et al*., 2004), as well as in fibroblasts of these mice having been subjected to mechanical stress (Lammerding *et al*., 2004). Additionally, apoptosis is also increased after RNAi of FACE1 (known as Zmpste24 in mice), the specific metalloprotease required for prelamin A processing towards maturation of lamin A (Gruber *et al*., 2005).

One of the putative functions of nuclear structural proteins, such as A-type lamins, is to interact with the genome, in order to influence genome function (Bridger *et al*., 2007; Maraldi *et al*., 2006). In cells derived from laminopathy patients it has been observed that heterochromatin is displaced from the nuclear envelope (Sabatelli *et al*., 2001; Sewry *et al*., 2001; Capanni *et al*., 2003; Fidzianska & Hausmanowa-Petrusewicz, 2003; Goldman *et al*., 2004; Columbaro *et al*., 2005; Filesi *et al*., 2005; Scaffidi & Misteli, 2005) and this is also apparent in mice with *Lmna* mutations (Arimura *et al*., 2005) and in *Lmna* null mice (Sullivan *et al*., 1999; Nikolova *et al*., 2004). Further, this phenomenon has also been observed in cells with *EMD* mutations (Ognibene *et al*., 1999). Others have observed alterations to histone methylation regulating heterochromatin in laminopathy cells (Scaffidi & Misteli, 2005; Shumaker *et al*., 2006). To test the hypothesis that A-type lamins and/or emerin are involved in genome behaviour we used a chromosome-positioning assay. We have found that genome organization is altered in cells carrying *LMNA* mutations or a mutation in the *EMD* gene. Most interestingly, the pattern of chromosome positioning mimics the chromosome positioning found in normal nonproliferating cells (Bridger *et al*., 2000; Mehta *et al*., in preparation). We assessed the amount of micronucleation present within these cultures. We found that primary laminopathy fibroblast cultures and an X-EDMD cell line contain variable fractions of micronucleated cells, the highest incidences correlating well with mutations in the tail region of lamin A. Similarly, fractions of cells in apoptosis are high in all laminopathy cultures with the highest incidences in those cultures with highest levels of micronucleation.

Thus, we have established that in proliferating fibroblasts containing mutations in *LMNA* and *EMD*, there is perturbation to normal genome behaviour giving nonproliferating characteristics of genome organization, with micronucleation possibly leading to apoptosis.

Results

Table 1 lists the human dermal fibroblast (HDF) cell lines that have been employed in this study. They are heterozygous and homozygous primary cells from affected patients and carriers, as well as one patient that has mutations in both *LMNA* and *EMD* genes (Ben Yaou *et al*., 2004). The panel of cell lines was developed to represent a range of lamin A/C-related laminopathies as well as having cell lines with different mutations along the lamin A/C gene from amino acid residue 298 to 608, and one cell line with a heterozygous emerin mutation. Figure 1 displays a map of the different A-type lamin mutations along the lamin proteins. Supplementary Figure S1 displays the patterns of distribution of anti-A-type lamin and anti-emerin in these cells. The fraction of cells displaying each distribution is also shown in Supplementary Figure S1 K and L.

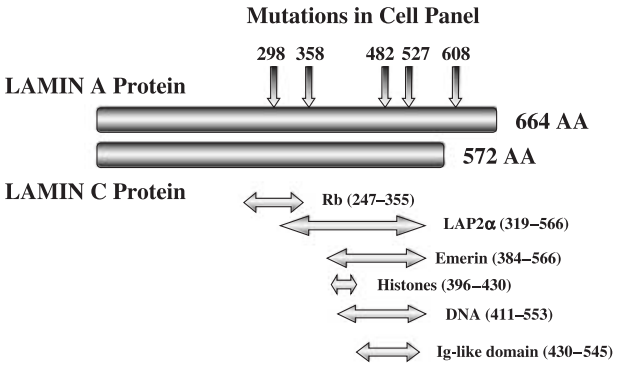

Fig. 1 Diagram of lamin A and C proteins. The position of all the mutations in *LMNA* for the cells used in this study are shown above the lamin A protein by vertical arrows. The regions of binding domains for Rb, DNA, emerin, LAP2α, histones (lamin C) and Ig-like domain (Krimm *et al*., 2002) are shown below the lamin A/C proteins by horizontal arrows (after Zastrow *et al*., 2004).

Table 1 Characterization of cell lines

Cell line	Cell type	Mutation	Disease phenotype	Reference
1HD	Primary HDF (P8)*	N/A	Normal	Bridger *et al*., 1998
2DD	Primary HDF (P15, P36)*	N/A	Normal	Bridger *et al*., 1993
R298C	Primary HDF (P10)*	*LMNA* R298C–/–	CMT2B	Unpublished data (N. Levy)
R298C–/–delK37y/–	Primary HDF (P10)*	*LMNA* R298C–/– & *EMD* del K37 Y/–	CMT2B+EDMD	Unpublished data (G. Bonne)
E358K	Primary HDF	*LMNA* E358K+/–	LGMD + atypical features	Mercuri *et al*., 2004
R482L	Primary HDF	*LMNA* R482L+/–	FPLD	Muchir *et al*., 2004
R527H–/–	Primary HDF	*LMNA* R527H–/–	MADA	Novelli *et al*., 2002
R527H+/–M	Primary HDF	*LMNA* R527H+/–	Unaffected, mother to R527–/–	Novelli *et al*., 2002
R527H+/–F	Primary HDF	*LMNA* R527H+/–	Unaffected, father to R527H–/–	Novelli *et al*., 2002
R527P	Primary HDF	*LMNA* R527P+/–	A-EDMD + FPLD	Muchir *et al*., 2004
AGO6297	Primary HDF (P22)*	*LMNA* G608G+/–†	HGPS	Coriel cell repository; Eriksson *et al*., 2003; Bridger & Kill, 2004
ED5364	Primary HDF (P12)*	*EMD* +/– specifics unknown	X-EDMD carrier	Unpublished (G. Morris)

+/– indicates the patient is heterozygous for the mutation, –/– indicates the patient is homozygous for the mutation.
*denotes passage number (where known) when fluorescence *in situ* hybridization (FISH) and immunofluorescence were performed.
†Mutation only affects lamin A.
'M' signifies mother and 'F' signifies father.
HDF, human dermal fibroblast; FPLD, Dunningan-type familial partial lipodystrophy; MADA, mandibuloacral dysplasia; HGPS, Hutchinson-Gilford progeria syndrome.

Genome organization is altered in primary laminopathy and X-EDMD human dermal fibroblasts and mimics nonproliferating fibroblasts

To test the hypothesis that A-type lamins and/or emerin are involved in translocating and anchoring chromosomes to the nuclear envelope, we analysed the nuclear localization of the gene-poor human chromosomes 4, 13, 18 and X in each of the cell lines using standard interphase fluorescence *in situ* hybridization (FISH) (Fig. 2). These chromosomes are known to be located at the nuclear periphery, abut the nuclear lamina (Boyle *et al*., 2001; possibly anchored by the lamina) (Foster & Bridger, 2005; Bridger *et al*., 2007). Analysis of chromosome position was performed by dividing the nucleus into five concentric shells of equal area for 50–60 nuclei (Croft *et al*., 1999; Bridger *et al*., 2000; Boyle *et al*., 2001; Meaburn *et al*., 2005). Shells 1 and 2 represent the area at the nuclear periphery, whereas shells 4 and 5 represent more the nuclear interior. The percentage of signal generated by the chromosome paint was measured in each of the five shells. To normalize the position data, the percentage of chromosome paint signal was divided by the percentage of DNA signal in each shell (Fig. 3 for data expressed graphically). Unpaired *t*-tests were performed to assess any significant differences in the normalised chromosome signal in each cell line, compared to the control cell line (1HD). The results are summarised in Table 2. A chromosome was described as being positioned towards the nuclear periphery if the chromosome signal after normalisation was skewed towards the peripheral shells (shells 1 and 2) (P), was distributed intermediately if a bell-shaped curve with a peak in shell 3 was observed (IM), was equally distributed if each shell contained similar amounts of normalised chromosome signal (E) and was described as internal if the chromosome signal was skewed towards the interior shells (shells 4 and 5) (I). Since chromosome positioning is different in nonproliferating nuclei as compared to proliferating nuclei (Bridger *et al*., 2000), the proliferation status of each nucleus was assessed by staining for the presence of pKi-67 (Fig. 2), an antigen found only in proliferating nuclei (Gerdes *et al*., 1984; Kill, 1996). PKi-67 has a number of distinct patterns in the proliferative cell cycle, three different patterns of speckled distribution can be discerned in early G1 (Bridger *et al*., 1998), with pKi-67 becoming only located at nucleoli in the rest of G1, S-phase and G2 (Verheijen *et al*., 1989a).

In normal control human dermal fibroblasts (1HD), the position of chromosome 18 was affected by the proliferation status of the cells, with chromosomes becoming located more internally in nonproliferating nuclei (Figs 2G and 3; Table 2). This loss of peripheral positioning was pronounced for chromosome 18 but was also seen to a lesser extent for chromosome 13 (Figs 2F and 3; Table 2). Interestingly, when chromosomes 4 and X were positioned in the control human dermal fibroblast (1HD) line they displayed little change in their nuclear positioning at the nuclear periphery, whether in proliferating or nonproliferating cells (Figs 2A,D,E,H and 3; Table 2). This demonstrates that different chromosomes may interact differently with specific nuclear structures and how they respond to signaled stimuli.

We also analysed the position of chromosomes 4, 13, 18 and X in our library of HDF cell lines with mutations in the *LMNA* and/or *EMD* genes. In all these mutant HDF cell lines chromosomes 4 and X were always positioned at the nuclear periphery in both proliferating and nonproliferating cells (Figs 2I,L,M,P and 3; Table 2), apart from chromosome X in R482L which has become more intermediate in its positioning (Fig. 3; Table 2). Most interestingly, when the nuclear positions of chromosomes

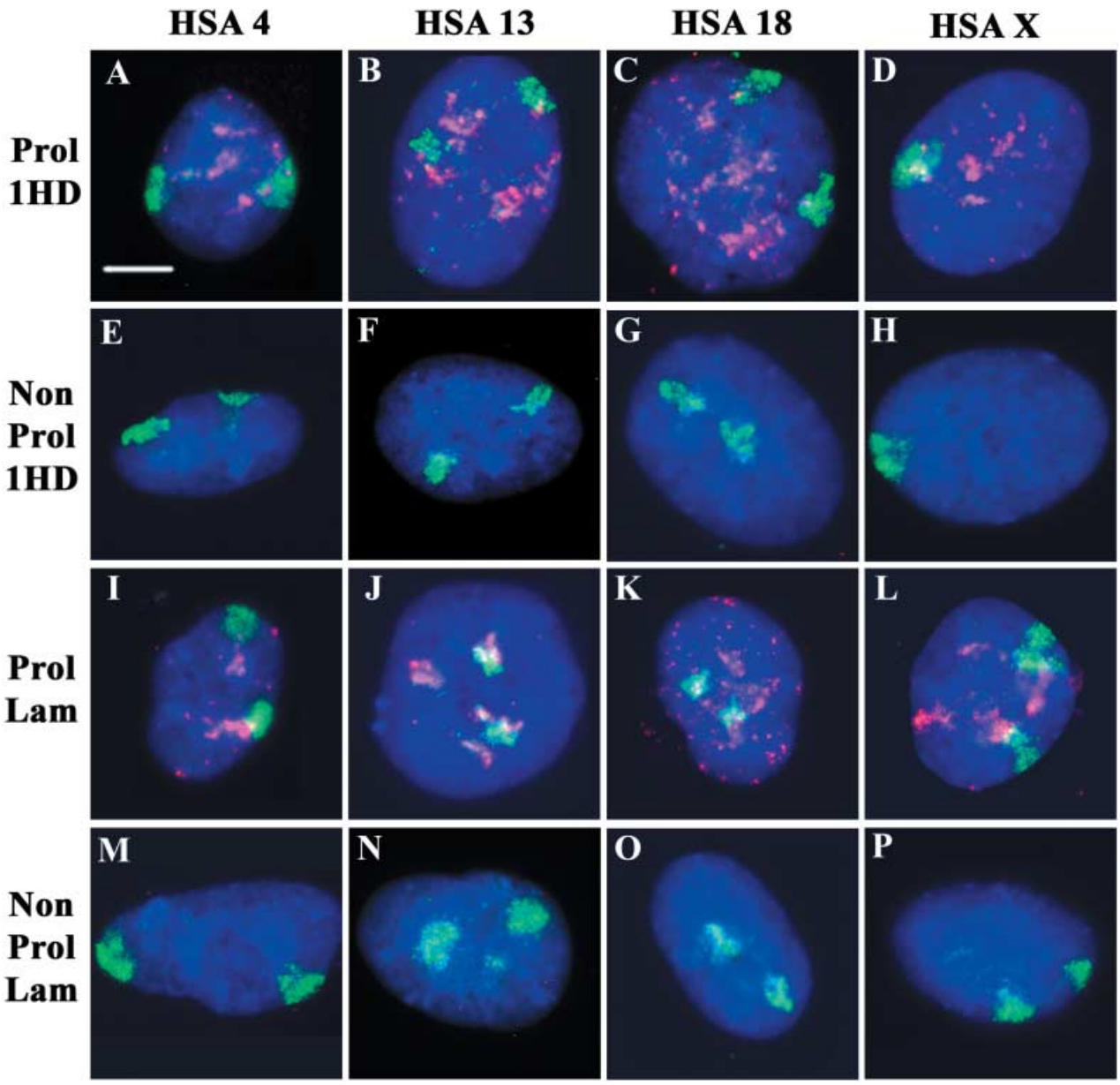

Fig. 2 Representative images of nuclear positioning of chromosomes 4, 13, 18 and X in proliferating and nonproliferating control and laminopathy human dermal fibroblasts (HDF). Methanol: acetic acid-fixed nuclei were hybridized with whole human chromosome paints (green), stained for the presence of a proliferation marker (pKi-67 red) and counterstained with DAPI (blue). A–D display representative images of Ki-67-positive 1HD nuclei, chromosomes 4, 13, 18 and X, respectively. E–H display representative images of nonproliferating (Ki-67 negative) 1HD nuclei, chromosomes 4, 13, 18 and X, respectively. I–P, primary mutant laminopathy HDFs, whereas I–L display proliferating nuclei, and M–P, nonproliferating nuclei. I, M – E358K, J – AGO6297 and N – R527P+/–, K, O – R298C, L, P – ED5364. Scale bar = 5 μm.

13 and 18 were determined in proliferating laminopathy cells and an X-EDMD cell line, chromosomes 13 and 18 were located away from the nuclear periphery, most often in the nuclear interior or for chromosome 13 in an intermediate location in R482L or R527H–/– (Figs 2J,K,R,S and 3; Table 2). This is a similar nuclear location that these chromosomes take in nonproliferating cells (Figs 2F,G and 3; Table 2). Despite having lamin A/C and emerin present at the nuclear envelope (NE), in similar amounts, in the majority of nuclei, these mutations lead to a pronounced effect on the location of a subset of chromosomes in the majority of cells.

Thus, genome organization is affected in cells derived from heterozygotes or homozygotes equally but it seems not to be correlated with whether A-type lamin and/or emerin can be detected at the nuclear periphery (also see Meaburn *et al.*, 2005).

Increased micronuclei in patients with FPLD and MADA and an X-EDMD carrier

Abnormal nuclear morphology is common to laminopathy or *LMNA* null cell lines (Hutchison & Worman, 2004) and in senescent

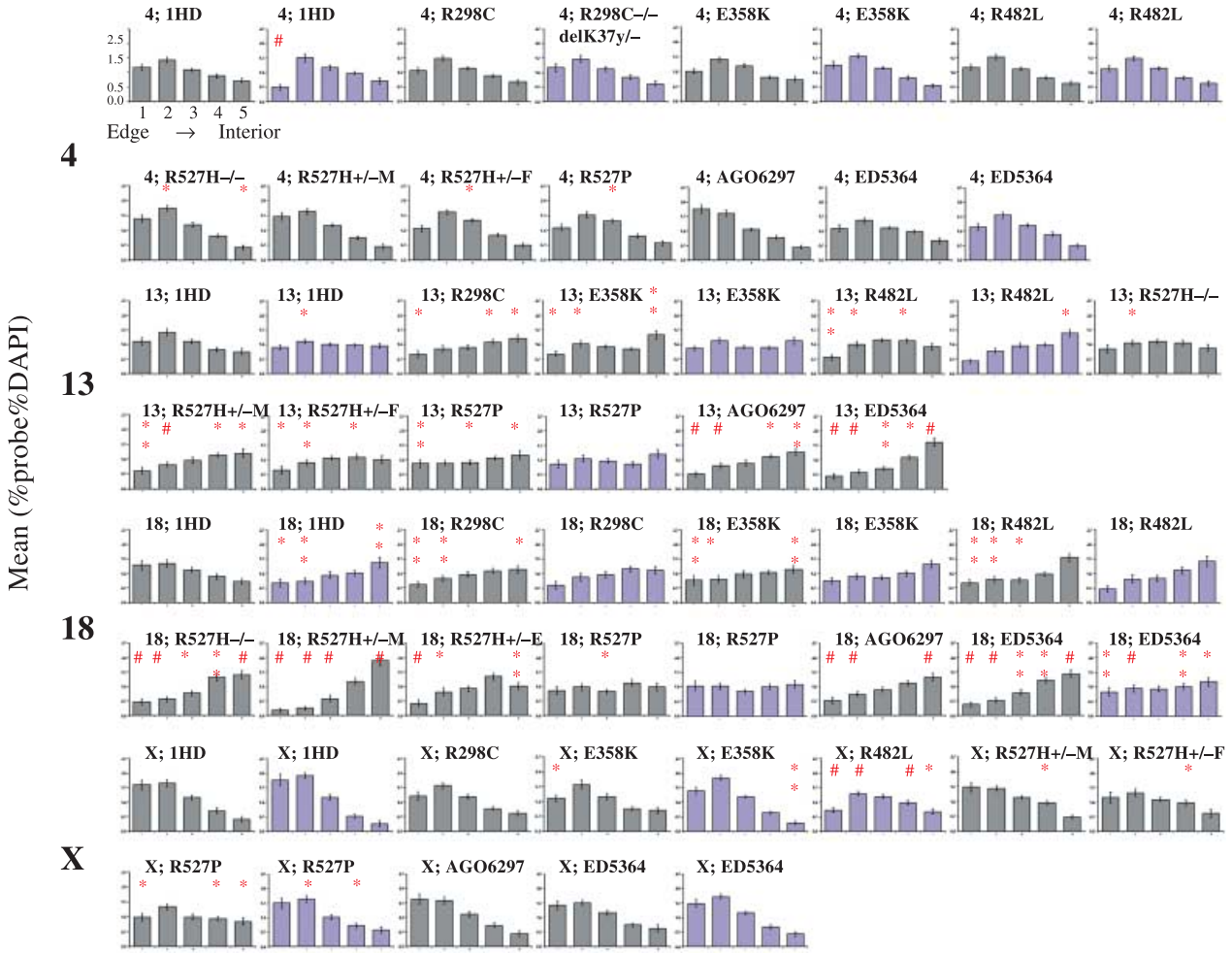

Fig. 3 Graphs to demonstrate that genome organization is affected by *LMNA* and *EMD* mutations in laminopathy human dermal fibroblasts (HDF). Nuclei were submitted to erosion analysis (see Experimental procedures). The normalised amount of chromosome signal (*x*-axis) for each of the five shells (*y*-axis) was plotted as histograms. Error bars show standard error of the mean. Grey bars denote proliferating nuclei, Mauve bars denote nonproliferating nuclei. Fifty to 60 nuclei were analysed, with the following exceptions: R298C chromosome 18 nonproliferating $n = 46$, R482L chromosome 18, nonproliferating $n = 41$, R527P+/–chromosome X and nonproliferating $n = 42$. The number or letter above each graph demonstrates which chromosome has been analysed. Statistical difference is denoted above the bar for that shell by * ($P < 0.05$), ** ($P < 0.005$) or # ($P < 0.0005$), as assessed by unpaired, unequal variances, two-tailed Students *t*-test, to the control cell line (1HD) in the case of proliferating data, or the proliferating data of the same cell line in the case of the nonproliferating graphs, except in the case of R482L, which was compared to 1HD nonproliferating.

cells (Bridger & Kill, 2004). Thus, this intimates that laminopathy cell lines may display an increased genomic instability (Liu *et al.*, 2005). Abnormal nuclei with micronuclei have been observed previously for HGPS cells (Bridger & Kill, 2004) and when the endoprotease responsible for cleaving prelamin A is knocked down by RNAi in human cells (Gruber *et al.*, 2005). Thus, we wanted to assess whether other laminopathy cells also displayed an increase in micronucleation.

Human dermal fibroblasts were grown on cover slips until approximately 70% confluent, fixed by either methanol:acetone or 4% paraformaldehyde, stained with 4′,6-diamidino-2-phenylindole (DAPI) and counter stained with antilamin A/C or anti-emerin and anti-pKi67. In this assay, micronuclei were only counted if they were separated from the main nucleus therefore only micronuclei and not blebs were scored. Representative images of and the fraction of cells displaying micronucleation are shown in Fig. 4 and Table 3, respectively. Interestingly, some micronuclei were positive for pKi67 while the main nucleus was negative. This could imply that these micronuclei were created while the cell was still proliferating and there is no system for breaking-down pKi67 inside the micronuclei but there is in the main nucleus. There are a number of micronuclei (~45%, combined for all laminopathy cells and an X-EDMD cell line, SD 16.5%) that are negative for pKi67 but the main nucleus is still positive – this implies that the micronuclei are not made at mitosis when all the chromosomes are coated with pKi67 (Verheijen *et al.*, 1989b), but during interphase, which maybe an important insight into the behaviour of the genome in laminopathies, X-EDMD and senescence/quiescence.

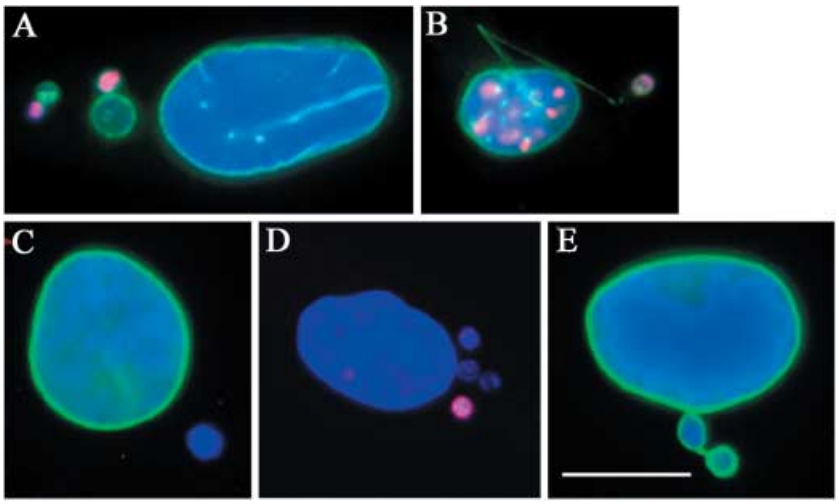

Fig. 4 Laminopathy cells displaying micronucleation. Laminopathy cells were either stained with antilamin A/C antibodies (A, B, E) or anti-emerin antibodies (C, D) (green) in combination antipKi-67 (red) and counterstained with 4′,6-diamidino-2-phenylindole (DAPI). A small range of representative images is shown in this figure – A, B = R527–/–; C, E = R298C–/–delK37y/–; D = ED5364. Micronuclei are seen that are still connected with the main nucleus (B, E), some micronuclei display positive staining for pKi-67 when the main body of the nucleus is negative (A, D). A number of micronuclei are negative for A-type lamin and/or emerin but are associated with a nucleus that is positively stained (C). Scale bar = 10 μm.

Table 2 Positioning of chromosomes 4, 13, 18 and X in normal and mutant cell lines

	Chromosome 4*		Chromosome 13*		Chromosome 18*		Chromosome X*	
Cell line	Proliferating†	Nonproliferating‡	Proliferating†	Nonproliferating‡	Proliferating†	Nonproliferating‡	Proliferating†	Nonproliferating‡
1HD	P	P	P	E	P	I	P	P
R298C	P	ND	I	ND	I	I	P	ND
R298C–/–delK37y/–	ND	P	ND	ND	ND	ND	ND	ND
E358K	P	P	E/I	E	I	I	P	P
R482L§	P	P	IM/E	I	I	I *n* = 41	ND	P/IM
R527H–/–	P	ND	E/I	ND	I	ND	ND	ND
R527H+/–M	P	ND	I	ND	I	ND	P	ND
R527H+/–F	P	ND	E/I	ND	I	ND	P	ND
R527P+/–	P	ND	E/I	E/I	E	E	P	P *n* = 42
AGO6297	P	ND	I	ND	I	ND	P	ND
ED5364	P	P	I	ND	I	I	P	P *n* = 48

*The position of the chromosome from each cell line, based on results as shown in Fig. 4. *n* = 50–60 unless otherwise stated.
†Nuclei positive for cell proliferation marker, pKi-67.
‡Nuclei negative for pKi-67.
§The majority of R482L's proliferating cells were only weakly positive for pKi-67.
'P' denotes the chromosome in a peripheral position (chromosome enrichment at the nuclear edge, shells 1 and 2), 'I' denotes an internal (chromosome enrichment at the centre of the nuclei, shell 5) positioning of the chromosome, 'IM' denotes an intermediate positioning for the chromosome within the nuclei (chromosome enrichment in shell 3), 'E' denotes chromosome signal distributed evenly through out all shells. 'ND' indicates where the position of the chromosome has not been determined.

A significant increase in cells with micronuclei was detected in the laminopathy cell lines R482L (11.9%, $P < 0.001$) and R527H–/– (7.3%, $P < 0.001$), from that observed for senescent normal HDF (2.6%) and in the X-EDMD line ED5364 (3.6%, $P < 0.05$), from that observed for young normal HDF (0.7–1.3%).

Accordingly, from the analysed cell lines, only cells derived from Dunningan-type familial partial lipodystrophy (FPLD) (R482L) or MADA (R527H–/–) (Table 3) and the X-EDMD line ED5364 revealed a significant increase in micronucleation. For the remaining laminopathy cell lines, the percentage of cells containing micronuclei did not differ significantly from that of old or young normal HDF. Both lines from healthy carriers heterozygous for the MADA mutation (R527H+/–F and R527+/–M) were within the range of young passage control HDF. These data reveal that *LMNA* mutation R298C is not associated with an increase in micronucleation, whereas the *LMNA* mutations in R482L and R527H–/– patients are associated with an increase in micronuclei. This, thereby, suggests a mutation or disease-specific aspect to the A-type lamin/emerin-associated reduction in stable behaviour of the genome.

Increased fraction of cells displaying apoptosis in all laminopathy and X-EDMD cells tested with massive increases in FPLD and MADA cells

We have shown previously that there is an increase in the percentage of apoptotic cells in cultures derived from HGPS patients compared with normal cultures (Bridger & Kill, 2004).

Table 3 Comparison of the fraction of mutant and control human dermal fibroblast (HDF)-containing micronuclei

Cell line	Passage	Percentage of cells with MN (cell with MN/total number of cell counted)	χ^2 to young normal HDF	χ^2 to senescent normal HDF
1HD (WT)	10	0.7% (6/896)	NSD	NSD
2DD (WT)	15	1.3% 17/1298	NSD	NSD
2DD (WT)	36	2.6% 26/1010	NSD	–
R298C (L)	10	1.4% (32/2221)	NSD	NSD
R298C–/–delK37y/– (L)	10	1.5% (17/1148)	NSD	NSD
E358K (L)	a	2.1% (66/3119)	NSD	NSD
R482L (L)	a	11.9% (233/1966)	$P < 0.001$	$P < 0.001$
R527H–/– (L)	a	7.3% (146/2001)	$P < 0.001$	$P < 0.01$
R527H+/–M (C)	a	1.0% (6/581)	NSD	NSD
R527H+/–F (C)	a	1.2% (9/763)	NSD	NSD
R527P+/– (L)	a	2.3% (43/1850)	NSD	NSD
AGO6297 (L)	20	2.1% (18/841)	NSD	NSD
ED5364 (C)	12	3.4% (29/854)	$P < 0.05$	NSD

WT, wild-type (normal), L, laminopathy cell line; C, Carrier line (see Table 1).
'a' is used in place of passage number, where passage number is unknown but denotes the passage at which samples were harvested for 2D fluorescence *in situ* hybridization (FISH), and are a presenescent culture.
χ^2, Statistical significance was determined by Yates correlate χ^2 analysis.
Mutant HDF cell lines were compared to either the average of the young passages of normal HDF (0.7%) or the senescent normal HDF (2.6%).

Table 4 Fraction of cells displaying apoptosis

Cell line	Apoptotic index
1HD	1.1%
1HD + UV	18%
R298C	18.9%
E358K	11.4%
R482L	43.5%
R527H+/–F	11%
R527H–/–	36%
ED5364	13.4%

The apoptotic indices for a number of laminopathy cell lines and an *EMD* = +/– cell line are shown.
1HD is used as a control cell line with its irradiation by UV as a positive control.
Apotosis was measured using a flow cytometry after annexin V and propidium iodide staining.
Cells were harvested for the apoptosis study 2 passages after fluorescence *in situ* hybridization (FISH) was performed.

Therefore, we predicted that cell lines derived from other laminopathies would also show increases in levels of apoptosis. We submitted a number of cell lines from our panel to an apoptotic analysis using Annexin V and propidium iodide staining and flow cytometry (Table 4). Cells were harvested within two passages of when the cells were fixed for FISH. As predicted all laminopathy cells analysed (R298C, E358K, R482L, R527–/–F, R527H–/–) show significantly increased percentages of cells undergoing apoptosis compared with normal fibroblasts. Even ED5364 with a mutation in emerin displayed an increased level of apoptosis (13.4%). Surprisingly, even the heterozygous cell line, R527H+/–F, shows high rates of apoptosis (11%) although not as high as the homozygote individual R527H–/– (36%). The largest increases are found in cell lines derived from FPLD and MADA patients (R482L and R527–/–, respectively). These are two of the cell lines that show significant increases in micronucleus formation. Thus it is possible that the two events are related. However, even cell lines that do not show increased micronucleation, do have increased levels of apoptosis (R298C, E358K, R527+/–F). It is interesting to note that both FPLD and MADA are associated with premature aging (Filesi *et al*., 2005; Vigouroux & Capeau, 2005).

Proliferating laminopathy cell lines are negative for pRB form normally associated with proliferating cells

In proliferating laminopathy fibroblasts, as determined by pKi-67 staining, aspects of genome distribution were reminiscent of normal nonproliferating cells. One interpretation of this is that mutation in A-type lamin permits an uncoupling of a normally linked cell cycle signaling pathway. Since pRb is complexed with A-type lamins (Zastrow *et al*., 2004) and is central in initiating cellular senescence in combination with p16 (Thomas *et al*., 2003; Itahana *et al*., 2004), we assessed the fraction of cells displaying forms of pRb associated with all cells and with only proliferating cells. For this we employed two antibodies, one that reacted with both unphosphorylated and hyperphosphorylated forms of pRb (Ab-11) (Fig. 5A,C,D,F), and one that reacted with Rb phosphorylated at serine residue 795 (Clone pRb-10), reacting with the modified Rb found in the proliferative cell cycle (Fig. 5G,I). Lamin A binds pRb110 between amino acid residues 247 to 355 (Ozaki *et al*., 1994). Therefore, in our comparison we chose a cell line with a mutation in the Rb-binding site of lamin A (R298C), a cell line with a mutation just outside the Rb-binding site in lamin A (E358K) and a cell line with a mutation distant from the Rb-binding site (R527H–/–). We used normal fibroblasts as a control along with ED5364, an X-EDMD carrier. As before

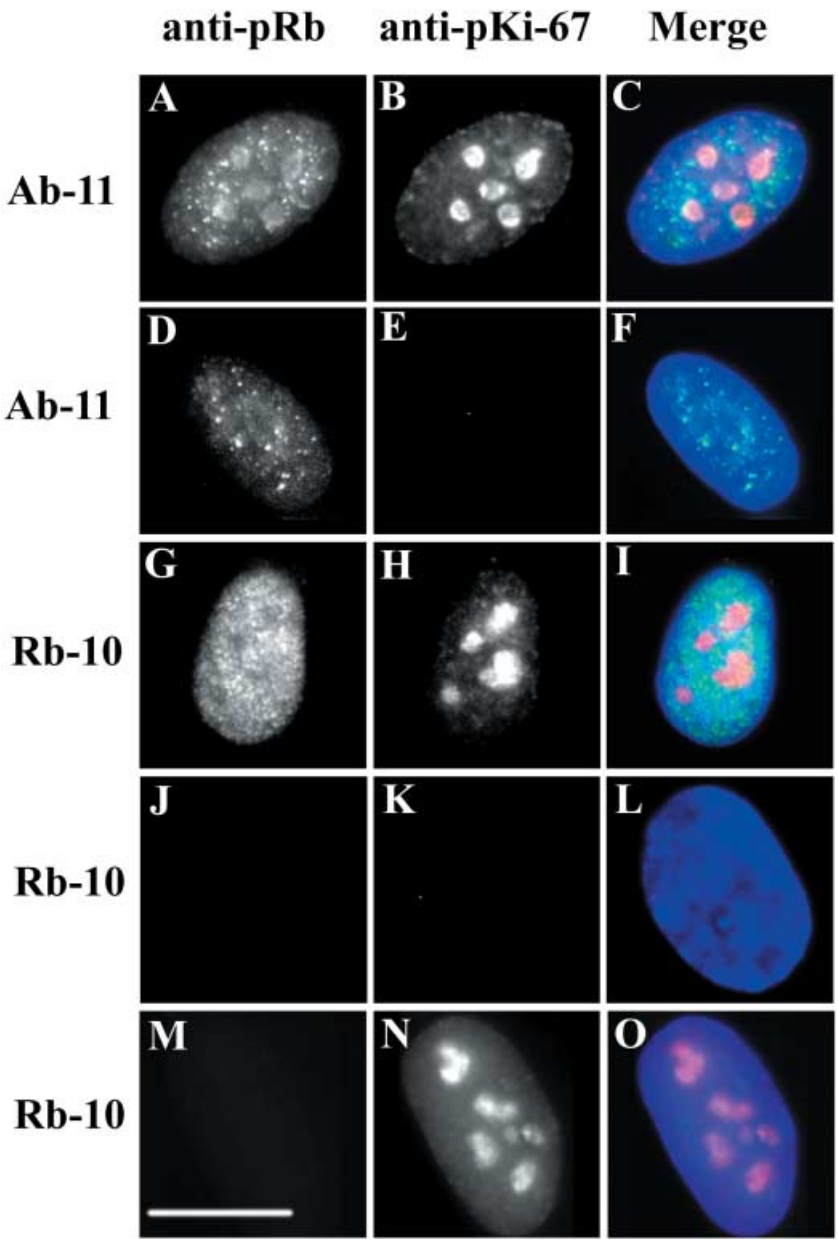

Fig. 5 Distribution of anti-Rb in proliferating and nonproliferating laminopathy cells. Paraformaldehyde (4%) fixed control and laminopathy human dermal fibroblasts were co-stained with anti-pKi67 antibodies (second column, red in third column) to reveal all proliferating cells and either anti-Rb ab-11 against phosphorylated and unphosphorylated forms of Rb (A, D) or clone Rb-10 reacting against pRb phosphoylated on ser 795 associated with proliferative cell cycle (first column, green in third column) (G, J, M). The third column displays a merged image of the anti-pRb staining (green), anti-pKi-67 (red) staining and a 4′,6-diamidino-2-phenylindole (DAPI) counter stain (blue). Representative nuclei of control cells are displayed in A–C and G–I and laminopathy cells are displayed in D–F and J–O. Scale bar = 10 μm.

we used pKi-67 positivity as an indicator of proliferative state. In normal cell cultures 90% of pKi-67 positive cells were also positive for Ab-11 (Table 5, Fig. 5A–C). Using Ab-10, ~60% of normal pKi-67 positive cells displayed staining with this antibody, indicating that this fraction of proliferating cells contained active pRb phosphorylated on ser 795. By inference 30% of Ki-67 positive cells contained only the form of pRb associated with nonproliferating cells. The fraction of cells within the laminopathy cultures that are pKi-67 positive and Ab-11 positive ranged from 77–99% (Table 5). These values are not significantly different from control cells (Yates χ^2 test). In contrast, the fraction of pKi-67 positive cells that were also positive for Ab-10 varied from 10 to 42% (Fig. 5G–H), which is significantly different from the control cell line. By inference, it appears that the laminopathy cultures assessed contain high fractions of proliferating cells with the active form of Rb found in nonproliferating cells. Interestingly, the cell line with the lowest fraction of cells containing active Rb is R527H–/–, with a mutation most distant from the Rb-binding site in lamin A but is within the DNA-binding site (Fig. 1).

Discussion

Since proteins of the nuclear lamina are postulated to have a role in genome behaviour and stability, we wanted to test the hypothesis that chromosomes would alter their characteristics and behaviour in cells with mutations in A-type lamins and emerin. Further, we hoped to determine which regions of the lamin A protein were responsible for any alterations to genome

Table 5 Fraction of cells positive for anti-Rb

	% of proliferating cells pKi-67 positive anti-Rb positive		
Cell line	Clone Rb ab-11 (total Rb)	Clone Rb-10 (Rb associated with the proliferative cell cycle)	Total number of cells displaying pRb associated with nonproliferation
1HD	90.0 ± 2.2	59.3 ± 1.7	30.7
R298C	96.7 ± 0.6	31.7 ± 3.0	65.0
E358K	93.3 ± 1.4	40.1 ± 6.2	53.2
R527H–/–	76.9 ± 1.2	10.4 ± 2.3	66.5
ED5364	98.9 ± 1.7	41.5 ± 6.6	57.4

Only cells positive for the proliferation marker pKi-67 were assessed for their presence or absence of anti-pRb staining with two different antibodies.
Clone Rb (ab-11) reacts with phosphorylated and unphosphorylated pRb and Clone Rb-10 reacts with phosphor-Rb (ser 795).
Total number of cells displaying pRb associated with nonproliferating cells is calculated by subtraction of the percentage positive for the proliferative form of Rb (phosphorylation on ser 795) from the percentage total Rb.
The percentage of cells that were positive for pKi-67 in the culture were 60% for 1HD, 40% for R298C, 42% for E358K, 34% for R527H–/– and 27% for ED 5364.

behaviour. Thus, we analysed the nuclear position of chromosomes normally located at the nuclear periphery in a panel of dermal fibroblast nuclei derived from individuals harboring various mutations in A-type lamins and one in emerin.

The positioning of chromosomes observed in the proliferating laminopathy cells and a carrier X-EDMD cell line was altered with two smaller chromosomes normally found at the nuclear periphery being located more towards the nuclear interior and the position of two larger chromosomes unchanged at the nuclear periphery, apart from chromosome X in nonproliferating R482L cells. In these cells the X chromosome is slightly removed from the nuclear edge (Fig. 3). Cells with this same mutation are being investigated further for disturbed genome organization.

Our analyses revealed that genome organization was affected in all proliferating laminopathy cells analysed, even in heterozygotes, wherever the lamin A mutation was located in the *LMNA* gene (see Fig. 1) and when cells were displaying what appeared to be a normal A-type lamina at the nuclear envelope (see Supplementary material). This then begs the question of how important chromosome positioning is to normal development since asymptomatic carriers displayed altered genome organization, as did the patient cells. What is clear, however, is that nuclear structural proteins A-type lamins and emerin are involved in genome behaviour in fibroblast cells.

A similar alteration in genome organization was revealed in all patient cells, whatever disease the donors were diagnosed with. It should be noted that the same laminopathy syndromes can be due to mutations at different regions of the lamin A gene and that families carrying the same mutation can display a range of different laminopathies (Jacob & Garg, 2006; Rankin & Ellard, 2006; and references therein). We have not yet assayed for alterations in genome organization in cells with mutations at the head region of lamin A, i.e. such as in atypical Werners syndrome (Chen *et al*., 2003).

The nuclear positioning of chromosomes in these proliferating laminopathy cells mimics the chromosome positioning found in normal nonproliferating senescent and quiescent cells (Bridger *et al*., 2000; Mehta *et al*., in preparation). Thus, proliferating laminopathy cells display at least one characteristic of nonproliferating cells. In addition, senescent cells are also characterized by their inability to phosphorylate pRb and to generate active forms of Rb (Stein & Dulic, 1998). Our analysis of pRb in laminopathy cultures reveals high proportions of cells containing the form of pRb (phosphorylated on Ser-795) associated with the proliferative cell cycle despite being positive for pKi-67, a definitive marker for proliferation (Fig. 5, Table 5). Thus, proliferating laminopathy cells can also resemble nonproliferating normal cells by this criterion as well.

This also begs the question of whether A-type lamins and emerin are involved in normal senescence and quiescence, and indeed Scaffidi & Misteli (2006) presented evidence that the cryptic splice site mutated in many HGPS cell lines can be used in cells derived from healthy individuals. Moreover, as mice age there is a reduced expression of lamin A/C in osteoblasts, chondrocytes and bone marrow (Duque & Rivas, 2006). Filesi *et al*. (2005) found that fibroblasts derived from the aged patients with MADA revealed a more pronounced irregularity in envelope organization and heterochromatin distribution, suggesting that lamins are directly involved in chromatin organization and mechanical integrity of the nucleus and that this is crucial to maintain cell and tissue integrity during aging. Our data add credence to this development that younger laminopathy and X-EDMD cells may behave like normal senescent cells and that nuclear envelope proteins may well be involved in the normal aging process. Further, we predict that the change in chromosome position in proliferating laminopathy fibroblasts is not just simply due to loss of anchorage at the nuclear envelope but that there has been an uncoupling of pathways involved in cellular proliferation that act through A-type lamins and/or emerin. This requires further investigation in both symptomatic and unaffected carriers since all cell lines display an alternative location for the smaller chromosomes. Since lamin A may have many functions, it is possible that we have uncovered a consequence of affecting a role in proliferation, which when combined with the effects of specific mutation on the differentiation of distinct cell types leads to different disease phenotypes.

It is not clear at this stage in our investigations whether the altered positioning of specific chromosomes affects gene expression and whether the chromosomes that move towards the nuclear interior have less histone methylation as observed for the X chromosome in the recent study in HGPS cells by Goldman and colleagues (Shumaker *et al*., 2006). However, the inactive X in the Goldman study does not appear to be located away from the nuclear edge in HGPS or cells transfected with the gene for progerin (the protein formed in HGPS patients with G608 mutation), which is confirmatory of our data for the X chromosomes. However, two of the cell lines employed in this study have been used in microarray analyses to assess any changes to gene expression and in the HGPS cell line AG06297 and MADA cell line R527H–/–, alterations to gene expression as compared to normal cells have been observed (Ly *et al*., 2000; Amati *et al*., 2004, respectively). Interestingly, when the aberrant splicing that occurs in HGPS with G608 mutation is corrected with an oligonucleotide morpholino, expression of certain genes becomes more normal (Scaffidi & Misteli, 2005).

There has also been evidence of genomic instability in some laminopathies (see Corso *et al*., 2005; Liu *et al*., 2005) that could cause loss of genetic material and catatrosphic events such as apoptosis. We wished to ascertain whether there was any indication of unstable genomes in the laminopathy cell lines and the X-EDMD cells by scoring the level of micronucleation in the cultures, a feature prominent in cells with genomic instability (Fenech, 2000) and obvious in cells towards the end of their lifespan (Wojda & Witt, 2003). Due to the connection of micronucleation with apoptosis and given that apoptosis could potentially account for tissue degeneration in progeria (Bridger & Kill, 2004), we also assessed the fractions of laminopathy cells in our panel undergoing apoptosis. Interestingly, the two laminopathy cell lines that displayed increased levels of micronuclei in this study showed the highest levels of apoptosis. These cell lines are derived from MADA (R527H–/–) and FPLD (R482L) patients. The former display aspects of premature aging (Filesi *et al*., 2005) and lipodystrophy is found in premature aging (Vigouroux & Capeau, 2005). Their mutations are reasonably close together on the proteins at residues 482 and 527, respectively, in the tail region encompassed by the DNA-binding motif from residues 411 to 553 (Stierle *et al*., 2003), which does not contain mutations for any of the other cell lines analysed in this study. From our data, micronucleation does not appear to be a feature of laminopathies *per se*. Indeed, the fraction of cells displaying micronuclei in the other laminopathy cell lines is very similar to normal senescent cells. However, ED5364 *EMD* +/– line also has a significant increase in micronucleation, whereas R298C–/–delK37y/– does not. The asymptomatic heterozygote carriers for R527H–/+ did not show any increase in micronucleation above normal cells but did show higher levels of apoptosis than normal. The consequences of these observations for the heterozygotes are as yet unclear.

One important question to ask is how might any of the A-type lamin and emerin mutations lead to an uncoupling of proliferation and cell cycle arrest signals, given that we see proliferating cells displaying characteristics of nonproliferating cells. We know that A-type lamins have a putative role in cell cycle control, probably through interactions with the cell cycle regulator pRb (Ozaki *et al*., 1994; Markiewicz *et al*., 2002; Johnson *et al*., 2004; Bakay *et al*., 2006). In addition, A-type lamins have recently been demonstrated to be required for the stabilisation, correct location and therefore activity of pRb (Johnson *et al*., 2004). Indeed, *Lmna* null cells are phenotypically similar to Rb null cells, displaying rapid proliferation and aberrant cell cycle timing (Johnson *et al*., 2004). It has also been shown that lamin A/C and binding partner LAP2α are required for pRb nuclear tethering in intranuclear foci (Markiewicz *et al*., 2002). This binding may be important for pRb function as a cell cycle regulator, where it regulates gene expression required for the cell to progress to S-phase (Mancini *et al*., 1994). Since the intranuclear foci of A-type lamins, LAP2α and pRb probably also contain emerin, it is not surprising that A-type lamin mutations and emerin lead to deregulation of cell cycle events. Furthermore, a mutation of the LAP2α gene has been shown to be responsible for dilated cardiomyopathy (Taylor *et al*., 2005). PRb is also associated and functions with histone deacetylases (HDAC) that modify chromatin (Harbour & Dean, 2000), creating gene silencing. Trichostatin A treatment, which inhibits HDAC activity, in combination with mevinolin (inhibitor of farnesylation) improves the nuclear organisation of heterochromatin and morphology of HGPS cells with a G608G mutation (Columbaro *et al*., 2005). Much attention is being placed on Rb-containing pathways, however, Varela *et al*. (2005) have demonstrated that in Zmpste24 knock-out mice the cells display senescence characteristics with the p53 signaling being up-regulated.

The nuclear distributions of A-type lamins in the laminopathy cells are barely affected when compared to controls. This is surprising as in other studies (Boyle *et al*., 2001; Meaburn *et al*., 2005) it has been shown that genome organization is not altered in cultured immortal laminopathy lymphoblastoid cells even though A-type lamin and emerin distribution is severely perturbed (Meaburn *et al*., 2005). This adds to the evidence that laminopathic mutations affect certain tissues and specific cell lineages because cells derived from haemopoetic stem cells do not seem to be affected and that the tissues that are affected are derived from mesenchymal stem cells (Hutchison & Worman, 2004) that are represented here by dermal fibroblasts. This needs to be further clarified in affected nonimmortalized blood cells and immortalized fibroblasts.

How then do our findings help explain the pathology observed in patients suffering from laminopathy disease? Though it is not formally proven it is widely accepted that accumulation of senescent cells within tissues contributes to aging pathology (Patil *et al*., 2005). Thus our findings that the laminopathy cells behave to some degree as nonproliferating cells may be relevant for pathology in laminopathies. It has already been suggested that some laminopathies behave as premature aging syndromes (Benedetti & Merlini, 2004; Filesi *et al*., 2005; Broers *et al*., 2006; Mattout *et al*., 2006). However, our most significant finding reveals large increases in fractions of apoptotic cells in cultures.

Clearly, such a scenario in tissues would lead to tissue degeneration combined with proliferating cells becoming prematurely senescent as in HGPS due to hyperproliferation (Bridger & Kill, 2004) and then these proliferating cells further displaying nonproliferating-like behaviour.

In summary, fibroblasts derived from homozygous and heterozygous individuals with A-type lamin mutations and heterozygous individuals for emerin mutation display senescent/quiescent type characteristics at least for genome organization. Furthermore cells from all laminopathies tested had an increased fraction of cells in apoptosis and this could be a consequence of deregulated cell cycle control, possibly acting through Rb- or p53-associated pathways.

Experimental procedures

Cell culture

The HDF cell lines (see Table 1) were maintained in Dulbecco's modified eagles medium supplemented with 10% (v/v) fetal calf serum (FCS, Invitrogen, Paisley, UK), 20 mM glutamine (Invitrogen) and 2% (v/v) penicillin/streptomycin (Invitrogen), with the exception of AGO6297 which was grown in 15% FBS (v/v). All cells were cultured at 37 °C, in a humidified atmosphere containing 5% CO_2. All the cells used were grown in 10% serum and were not permitted to become confluent between passaging. Thus, any cells lacking pKi-67 staining should be senescent (Kill *et al*., 1994).

2D fluorescence *in situ* hybridization

Cells were harvested and swollen in hypotonic buffer (75 mM KCl) for 15 min at room temperature before fixation in ice-cold 3 : 1 (v/v) methanol/acetic acid. Cells were dropped onto humid slides and air dried before being aged at 70 °C for 1 h, or at room temperature for 2 days. After this, slides were dehydrated through an ethanol row (70%, 90%, 100%, 5 min each), air dried and prewarmed for 5 min at 70 °C before being placed in denaturing buffer [70% (v/v) formamide, 2× SSC (300 mM sodium chloride, 30 mM hydrous tri-sodium-citrate), pH 7; 70 °C] for 2 min. Slides were then immediately plunged into ice cold 70% ethanol, dehydrated in an ethanol row, air dried and kept warm.

Total chromosome DNA Probes (Qbiogene, Cambridge, UK) were prewarmed at 37 °C for 5 min, denatured at 72 °C for 10 min, followed by incubation at 37 °C for approximately 30–60 min. Some preparations used amplified flow-sorted HSA 18 by performing degenerate oligonucleotide primed polymerase chain reaction (DOP-PCR) and was subsequently labeled with biotin-16-dUTP (Boehringer Mannheim, Mannheim, Germany) and 8 μL PCR probe product, per slide, was combined with 7 μg C_0t_1 (Roche, Welwyn Garden City, UK) and 3 μg herring sperm (BDH, Poole, UK). The nuclei were hybridised with the probe for 36–60 h at 37 °C. The slides were then washed with wash buffer A [50% (v/v) formamide, 2× SSC, pH 7; preheated to 45 °C)], followed by wash buffer B (0.1× SSC, pH 7; preheated to 60 °C), both washes were performed at 45 °C, with three 5-min incubations each. The slides were then placed into 4× SSC, at room temperature. To detect the biotin-labeled probe, the slides were then incubated in an humidified chamber for 30 min at 37 °C, in 100 μL per slide of 2× SSC per 4% bovine serum albumin containing a 1 : 100 dilution of streptavidin FITC antibody (Amersham Life Sciences Ltd, Buckinghamshire, UK). The slides were then washed three times, for 5 min each in 4× SSC containing 0.05% Tween-20, at 42 °C. To determine if the HDF cells were proliferating or nonproliferating, the slides were then incubated for 2–3 h at 37 °C or overnight at 4 °C, with polyclonal rabbit anti-Ki67p (Novocastra, Newcastle upon Tyne, UK) antibody (diluted 1 : 1500 in 1% new-born calf serum/phosphate buffered saline (v/v, NCS/PBS). After PBS washes, the nuclei were incubated with Swine antirabbit TRITC or FITC (Dako UK Ltd., Cambridgeshire, UK; diluted 1 : 30 in 1% NSC/PBS) for 1 h at room temperature. Slides were washed again in PBS and counter stained by mounting in 1.5 μg mL^{-1} DAPI in Vectashield-mounting medium. Slides were examined under 100× oil-immersion objective, on a Leica fluorescent microscope (Leitz DMRB, Leica Microsystems Ltd., Milton Keynes, UK), and images of random nuclei were collected with a CCD camera (Sensys, Photometrics Inc, Huntington Beach, USA), using Quips pathvysion, SmartCapture VP V1.4 (Digital Scientific Ltd., Cambridge, UK). Simple erosion analysis was then performed on the captured images as described in Croft *et al*. (1999), briefly; 50–60 2D FISH images were run through a script written by P. Perry (MRC HGU, Edinburgh, UK) in IPLab Spectrum software. This separates the nuclei into five concentric shells of equal area eroded from the periphery (shell 1) to the interior (shell 5), recording DAPI and chromosome probe signal in each shell. Background was removed from the FISH signal by subtraction of the mean signal pixel intensity within the segmented nuclei. To normalise the probe signal the percentage of probe signal in each segment was divided by the percentage of the DAPI signal (total DNA) in that segment. Error bars on graphs denote +/– standard error of the mean. Statistical analysis was performed with the unpaired, unequal variances, two-tailed Students *t*-test, using Excel software.

Indirect immunofluorescence

Human dermal fibroblast cells of a similar passage number to that used in the 2D FISH experiments were grown on sterile cover slips and washed in PBS. Cells were fixed in either ice-cold methanol: acetone [1 : 1 (v/v)] for 10 min at 4 °C, or 4% (w/v) paraformaldehyde in PBS for 10 min at room temperature, followed by a wash in PBS. After this the paraformaldehyde-fixed cells were further treated with 1% (v/v) Triton-X 100 in PBS for 10 min at room temperature, followed with a PBS wash. Primary antibodies were incubated at 4 °C overnight or for 1 h at room temperature [mouse monoclonal antilamin A/C (Novocastra) diluted 1 : 10; mouse monoclonal anti-Emerin (Novocastra) diluted 1 : 20; rabbit antipKi-67 (Novocastra) 1 : 1000], mouse

monoclonal anti-Rb (ab-11) (Oncogene Research Products) 1 : 200 and mouse monoclonal anti-Rb clone Rb-10 (pS795) (Sigma-Aldrich Company Ltd., Dorset, UK) diluted 1 : 1000. The cover slips or slides were then washed in PBS. Cells were then incubated for 1 h, at room temperature, in donkey antimouse FITC or Cy3 (Jackson Immunoresearch Laboratories, Cambridgeshire, UK, diluted 1 : 60). The cover slips or slides were then washed in PBS and rinsed in distilled water. Cells were counter stained by mounting in 1.5 $\mu g\ mL^{-1}$ DAPI in mounting medium (Vector Laboratories, Ltd, Peterborough, UK). Slides were viewed on Leica fluorescent microscope (Leitz DMRB).

Apoptosis

The fraction of cells undergoing apoptosis was determined as described in Bridger & Kill (2004). Briefly, adherent cells were harvested and resuspended in binding buffer (10 mM HEPES/NaOH, pH 7.5, containing 140 mM NaCl and 2.5 mM $CaCl_2$) at a concentration of 10^6 cells per mL. These cells were two passages later than those harvested for FISH experiments. The cell suspension was incubated with 0.5 $\mu g\ mL^{-1}$ Annexin V FITC conjugate (Sigma-Aldrich) and 2 $\mu g\ mL^{-1}$ propidium iodide solution (Sigma-Aldrich) for 10 min in the absence of light. Fluorescence was determined by flow cytometry using a Beckman Coulter Epics XL-MCL (Beckman Coulter, Buckinghamshire, UK). For a positive apoptotic control cells were subjected to 100 JM^2 and assayed after 30 min.

Acknowledgments

We thank Dr Paul Perry and Prof Wendy Bickmore (MRC HGU, Edinburgh) for use of the erosion analysis script and Dr Julio Masabanda, Brunel University for flow sorted template for human chromosomes 18. The authors also wish to acknowledge V. Mouly and the platform of human cell culture in Pitié-Salpétrière. This work was supported by awards to Joanna M. Bridger from Brunel University and Brunel University Progeria Research Fund and partly by grants from Italian Health Ministry, Italian Telethon, Instituto Superiore di Sanità to Giuseppe Novelli, a grant to Gisele Bonne from Association Française contre les Myopathies' (AFM) rare disorder network program (no. 10722) and an EU grant 'Nuclear Envelope-linked Rare Human Diseases: From Molecular Pathophysiology towards Clinical Applications' FP6-018690.

References

Alsheimer M, Liebe B, Sewell L, Stewart CL, Scherthan H, Benavente R (2004) Disruption of spermatogenesis in mice lacking A-type lamins. *J. Cell. Sci.* **117**, 1173–1178.

Amati F, Biancolella M, D'Apice MR, Gambardella S, Mango R, Sbraccia P, D'Adamo M, Margiotti K, Nardone A, Lewis M, Novelli G (2004) Gene expression profiling of fibroblasts from a human progeroid disease (mandibuloacral dysplasia, MAD No. 248370) through cDNA microarrays. *Gene Expr.* **12**, 39–47.

Arimura T, Helbling-Leclerc A, Massart C, Varnous S, Niel F, Lacene E, Fromes Y, Toussaint M, Mura AM, Keller DI, Amthor H, Isnard R, Malissen M, Schwartz K, Bonne G (2005) Mouse model carrying H222P-Lmna mutation develops muscular dystrophy and dilated cardiomyopathy similar to human striated muscle laminopathies. *Hum. Mol. Genet.* **14**, 155–169.

Bakay M, Wang Z, Melcon G, Schiltz L, Xuan J, Zhao P, Sartorelli V, Seo J, Pegoraro E, Angelini C, Shneiderman B, Escolar D, Chen YW, Winokur ST, Pachman LM, Fan C, Mandler R, Nevo Y, Gordon E, Zhu Y, Dong Y, Wang Y, Hoffman EP (2006) Nuclear envelope dystrophies show a transcriptional fingerprint suggesting disruption of Rb-MyoD pathways in muscle regeneration. *Brain* **129**, 996–1013.

Ben Yaou R, Toutain A, Babuty D, Demay L, Peccate C, Muchir A, Arimura T, Massart C, Deburgrave N, Leturcq F, Litim K, Rahmouni-Chiali N, Richard P, Recan D, Bonne G (2004) Heterogeneous clinical expression of *LMNA* and *EMD* mutations segregating in a single family. Pathophysiologic implications for nuclear envelope related disorders. *Neuromuscul. Disord.* **14**, 592.

Benedetti S, Merlini L (2004) Laminopathies: from the heart of the cell to the clinics. *Curr. Opin. Neurol.* **17**, 553–560.

Bengtsson L, Wilson KL (2004) Multiple and surprising new functions for emerin, a nuclear membrane protein. *Curr. Opin. Cell Biol.* **16**, 73–79.

Bione S, Maestrini E, Rivella S, Mancini M, Regis S, Romeo G, Toniolo D (1994) Identification of a novel X-linked gene responsible for Emery-Dreifuss muscular dystrophy. *Nat. Genet.* **8**, 323–327.

Boyle S, Gilchrist S, Bridger JM, Mahy NL, Ellis JA, Bickmore WA (2001) The spatial organisation of human chromosomes within the nuclei of normal and emerin-mutant cells. *Hum. Mol. Genet.* **10**, 211–219.

Bridger JM, Bickmore WA (1998) Putting the genome on the map. *Trends Genet.* **14**, 403–409.

Bridger JM, Kill IR (2004) Ageing of Hutchinson–Gilford progeria syndrome fibroblasts is characterised by hyperproliferation and increased apoptosis. *Exp. Gerontol.* **39**, 717–724.

Bridger JM, Boyle S, Kill IR, Bickmore WA (2000) Re-modelling of nuclear architecture in quiescent and senescent human fibroblasts. *Curr. Biol.* **10**, 149–152.

Bridger JM, Foeger N, Kill IR, Herrmann H (2007) The Nuclear Lamina – a Structural Framework involved in Genome Organisation. *FEBS J.* in press.

Bridger JM, Kill IR, Lichter P (1998) Association of pKi-67 with satellite DNA of the human genome in early G1 cells. *Chromosome Res.* **6**, 13–24.

Bridger JM, Kill IR, O'Farrell M, Hutchison CJ (1993) Internal lamin structures within G1 nuclei of human dermal fibroblasts. *J. Cell. Sci.* **104**, 297–306.

Broers JL, Ramaekers FC, Bonne G, Yaou RB, Hutchison CJ (2006) Nuclear lamins: laminopathies and their role in premature ageing. *Physiol. Rev.* **86**, 967–1008.

Capanni C, Cenni V, Mattioli E, Sabatelli P, Ognibene A, Columbaro M, Parnaik VK, Wehnert M, Maraldi NM, Squarzoni S, Lattanzi G (2003) Failure of lamin A/C to functionally assemble in R482L mutated familial partial lipodystrophy fibroblasts: altered intermolecular interaction with emerin and implications for gene transcription. *Exp. Cell Res.* **291**, 122–134.

Chen L, Lee L, Kudlow BA, Dos Santos HG, Sletvold O, Shafeghati Y, Botha EG, Garg A, Hanson NB, Martin GM, Mian IS, Kennedy BK, Oshima J (2003) LMNA mutations in atypical Werner's syndrome. *Lancet* **362**, 440–445.

Columbaro M, Capanni C, Mattioli E, Novelli G, Parnaik VK, Squarzoni S, Maraldi NM, Lattanzi G (2005) Rescue of heterochromatin organization in Hutchinson–Gilford progeria by drug treatment. *Cell. Mol. Life Sci.* **62**, 2669–2678.

Corso C, Parry EM, Faragher RG, Seager A, Green MH, Parry JM (2005) Molecular cytogenetic insights into the ageing syndrome Hutchinson-Gilford Progeria (HGPS). *Cytogenet. Genome Res.* **111**, 27–33.

Croft JA, Bridger JM, Boyle S, Perry P, Teague P, Bickmore WA (1999) Differences in the localization and morphology of chromosomes in the human nucleus. *J. Cell Biol.* **145**, 1119–1131.

Dechat T, Korbei B, Vaughan OA, Vlcek S, Hutchison CJ, Foisner R (2000) Lamina-associated polypeptide 2alpha binds intranuclear A-type lamins. *J. Cell. Sci.* **113**, 3473–3484.

Duque G, Rivas D (2006) Age-related changes in lamin A/C expression in the osteoarticular system: laminopathies as a potential new aging mechanism. *Mech. Ageing Dev.* **127**, 378–383.

Eriksson M, Brown WT, Gordon LB, Glynn MW, Singer J, Scott L, Erdos MR, Robbins CM, Moses TY, Berglund P, Dutra A, Pak E, Durkin S, Csoka AB, Boehnke M, Glover TW, Collins FS (2003) Recurrent de novo point mutations in lamin A cause Hutchinson-Gilford progeria syndrome. *Nature* **423**, 293–298.

Fenech M (2000) The *in vitro* micronucleus technique. *Mutat. Res.* **455**, 81–95.

Fidzianska A, Hausmanowa-Petrusewicz I (2003) Architectural abnormalities in muscle nuclei. Ultrastructural differences between X-linked and autosomal dominant forms of EDMD. *J. Neurol. Sci.* **210**, 47–51.

Filesi I, Gullotta F, Lattanzi G, D'Apice MR, Capanni C, Nardone AM, Columbaro M, Scarano G, Mattioli E, Sabatelli P, Maraldi NM, Biocca S, Novelli G (2005) Alterations of nuclear envelope and chromatin organisation in mandibuloacral dysplasia, a rare form of laminopathy. *Physiol. Genomics* **23**, 150–158.

Foster HA, Bridger JM (2005) The genome and the nucleus: a marriage made by evolution: Genome organisation and nuclear architecture. *Chromosoma* **114**, 212–229.

Gerdes J, Lemke H, Baisch H, Wacker HH, Schwab U, Stein H (1984) Cell cycle analysis of a cell proliferation-associated human nuclear antigen defined by the monoclonal antibody Ki-67. *J. Immunol.* **133**, 1710–1715.

Goldman AE, Moir RD, Montag-Lowy M, Stewart M, Goldman RD (1992) Pathway of incorporation of microinjected lamin A into the nuclear envelope. *J. Cell Biol.* **119**, 725–735.

Goldman RD, Shumaker DK, Erdos MR, Eriksson M, Goldman AE, Gordon LB, Gruenbaum Y, Khuon S, Mendez M, Varga R, Collins FS (2004) Accumulation of mutant lamin A causes progressive changes in nuclear architecture in Hutchinson–Gilford progeria syndrome. *Proc. Natl Acad. Sci. USA* **101**, 8963–8968.

Gotzmann J, Foisner R (2005) A-type lamin complexes and regenerative potential: a step towards understanding laminopathic diseases? *Histochem. Cell Biol.* **2**, 1–9.

Gruber J, Lampe T, Osborn M, Weber K (2005) RNAi of FACE1 protease results in growth inhibition of human cells expressing lamin A: implications for Hutchinson-Gilford progeria syndrome. *J. Cell Sci.* **118**, 689–696.

Gruenbaum Y, Margalit A, Goldman RD, Shumaker DK, Wilson KL (2005) The nuclear lamina comes of age. *Nat. Rev. Mol. Cell Biol.* **6**, 21–31.

Harbour JW, Dean DC (2000) Chromatin remodeling and Rb activity. *Curr. Opin. Cell Biol.* **12**, 685–689.

Hutchison CJ, Worman HJ (2004) A-type lamins: guardians of the soma? *Nat. Cell Biol.* **6**, 1062–1067.

Itahana K, Campisi J, Dimri GP (2004) Mechanisms of cellular senescence in human and mouse cells. *Biogerontology* **5**, 1–10.

Jacob KN, Garg A (2006) Laminopathies: multisystem dystrophy syndromes. *Mol. Genet. Metab.* **87**, 289–302.

Johnson BR, Nitta RT, Frock RL, Mounkes L, Barbie DA, Stewart CL, Harlow E, Kennedy BK (2004) A-type lamins regulate retinoblastoma protein function by promoting subnuclear localization and preventing proteasomal degradation. *Proc. Natl Acad. Sci. USA* **101**, 9677–9682.

Kill IR, Faragher RG, Lawrence K, Shall S (1994) The expression of proliferation-dependent antigens during the lifespan of normal and progeroid human fibroblasts in culture. *J. Cell Sci.* **107**, 571–579.

Kill IR (1996) Localisation of the Ki-67 antigen within the nucleolus. Evidence for a fibrillarin-deficient region of the dense fibrillar component. *J. Cell Sci.* **109**, 1253–1263.

Krimm I, Ostlund Gilquin B, Couprie J, Hossenlopp P, Mornon JP, Bonne G, Courvalin JC, Worman HJ, Zinn-Justin S (2002) The Ig-like structure of the C-terminal domain of lamin A/C, mutated in muscular dystrophies, cardiomyopathy, and partial lipodystrophy. *Structure* **10**, 811–823.

Kudlow BA, Kennedy BK (2006) Aging: progeria and the lamin connection. *Curr. Biol.* **16**, R652–R654.

Lammerding J, Schulze PC, Takahashi T, Kozlov S, Sullivan T, Kamm RD, Stewart CL, Lee RT (2004) Lamin A/C deficiency causes defective nuclear mechanics and mechanotransduction. *J. Clin. Invest.* **113**, 370–378.

Liu B, Wang J, Chan KM, Tjia WM, Deng W, Guan X, Huang JD, Li KM, Chau PY, Chen DJ, Pei D, Pendas AM, Cadinanos J, Lopez-Otin C, Tse HF, Hutchison C, Chen J, Cao Y, Cheah KS, Tryggvason K, Zhou Z (2005) Genomic instability in laminopathy-based premature ageing. *Nat. Med.* **11**, 780–785.

Ly DH, Lockhart DJ, Lerner RA, Schultz PG (2000) Mitotic misregulation and human ageing. *Science* **287**, 2390.

Mancini MA, Shan B, Nickerson JA, Penman S, Lee WH (1994) The retinoblastoma gene product is a cell cycle-dependent, nuclear matrix-associated protein. *Proc. Natl Acad. Sci. USA* **91**, 418–422.

Manilal S, Nguyen TM, Morris GE (1998) Colocalization of emerin and lamins in interphase nuclei and changes during mitosis. *Biochem. Biophys. Res. Commun.* **249**, 643–647.

Maraldi NM, Lattanzi G, Capanni C, Columbaro M, Merlini L, Mattioli E, Sabatelli P, Squarzoni S, Manzoli FA (2006) Nuclear envelope proteins and chromatin arrangement: a pathogenic mechanism for laminopathies. *Eur. J. Histochem.* **50**, 1–8.

Margalit A, Liu J, Fridkin A, Wilson KL, Gruenbaum Y (2005b) A lamin-dependent pathway that regulates nuclear organization, cell cycle progression and germ cell development. *Novartis Found. Symp.* **264**, 231–240.

Margalit A, Vlcek S, Gruenbaum Y, Foisner R (2005a) Breaking and making of the nuclear envelope. *J. Cell Biochem.* **95**, 454–465.

Markiewicz E, Dechat T, Foisner R, Quinlan RA, Hutchison CJ (2002) Lamin A/C binding protein LAP2alpha is required for nuclear anchorage of retinoblastoma protein. *Mol. Biol. Cell.* **13**, 4401–4413.

Mattout A, Dechat T, Adam SA, Goldman RD, Gruenbaum Y (2006) Nuclear lamins, diseases and aging. *Curr. Opin. Cell Biol.* **18**, 335–341.

McClintock D, Gordon LB, Djabali K (2006) Hutchinson-Gilford progeria mutant lamin A primarily targets human vascular cells as detected by an anti-Lamin A G608G antibody. *Proc. Natl Acad. Sci. USA* **103**, 2154–2159.

Meaburn KJ, Levy N, Toniolo D, Bridger JM (2005) Chromosome positioning is largely unaffected in lymphoblastoid cell lines containing Emerin and A-type lamin mutations. *Biochem. Soc. Trans.* **33**, 1438–1440.

Melcon G, Kozlov S, Cutler DA, Sullivan T, Hernandez L, Zhao P, Mitchell S, Nader G, Bakay M, Rottman JN, Hoffman EP, Stewart CL (2006) Loss of emerin at the nuclear envelope disrupts the Rb1/E2F and MyoD pathways during muscle regeneration. *Hum. Mol. Genet.* **15**, 637–561.

Mercuri E, Poppe M, Quinlivan R, Messina S, Kinali M, Demay L, Bourke J, Richard P, Sewry C, Pike M, Bonne G, Muntoni F, Bushby K (2004) Extreme variability of phenotype in patients with an identical missense mutation in the lamin A/C gene: from congenital onset with severe

phenotype to milder classic Emery-Dreifuss variant. *Arch. Neurol.* **61**, 690–694.

Muchir A, Medioni J, Laluc M, Massart C, Arimura T, van der Kooi AJ, Desguerre I, Mayer M, Ferrer X, Briault S, Hirano M, Worman HJ, Mallet A, Wehnert M, Schwartz K, Bonne G (2004) Nuclear envelope alterations in fibroblasts from patients with muscular dystrophy, cardiomyopathy, and partial lipodystrophy carrying lamin A/C gene mutations. *Muscle Nerve* **30**, 444–450.

Nikolova V, Leimena C, McMahon AC, Tan JC, Chandar S, Jogia D, Kesteven SH, Michalicek J, Otway R, Verheyen F, Rainer S, Stewart CL, Martin D, Feneley MP, Fatkin D (2004) Defects in nuclear structure and function promote dilated cardiomyopathy in lamin A/C-deficient mice. *J. Clin. Invest.* **113**, 357–369.

Novelli G, Muchir A, Sangiuolo F, Helbling-Leclerc A, D'Apice MR, Massart C, Capon F, Sbraccia P, Federici M, Lauro R, Tudisco C, Pallotta R, Scarano G, Dallapiccola B, Merlini L, Bonne G (2002) Mandibuloacral dysplasia is caused by a mutation in LMNA-encoding lamin A/C. *Am. J. Hum. Genet.* **71**, 426–431.

Ognibene A, Sabatelli P, Petrini S, Squarzoni S, Riccio M, Santi S, Villanova M, Palmeri S, Merlini L, Maraldi NM (1999) Nuclear changes in a case of X-linked Emery-Dreifuss muscular dystrophy. *Muscle Nerve* **22**, 864–869.

Ozaki T, Saijo M, Murakami K, Enomoto H, Taya Y, Sakiyama S (1994) Complex formation between lamin A and the retinoblastoma gene product: identification of the domain on lamin A required for its interaction. *Oncogene* **9**, 2649–2653.

Patil CK, Mian IS, Campisi J (2005) The thorny path linking cellular senescence to organismal ageing. *Mech. Ageing Dev.* **126**, 1040–1045.

Rankin J, Ellard S (2006) The laminopathies: a clinical review. *Clin. Genet.* **70**, 261–274.

Sabatelli P, Lattanzi G, Ognibene A, Columbaro M, Capanni C, Merlini L, Maraldi NM, Squarzoni S (2001) Nuclear alterations in autosomal-dominant Emery-Dreifuss muscular dystrophy. *Muscle Nerve* **24**, 826–829.

Scaffidi P, Misteli T (2005) Reversal of the cellular phenotype in the premature aging disease Hutchinson-Gilford progeria syndrome. *Nat. Med.* **11**, 440–445.

Scaffidi P, Misteli T (2006) Lamin A-dependent nuclear defects in human aging. *Science* **312**, 1059–1063.

Sewry CA, Brown SC, Mercuri E, Bonne G, Feng L, Camici G, Morris GE, Muntoni F (2001) Skeletal muscle pathology in autosomal dominant Emery-Dreifuss muscular dystrophy with lamin A/C mutations. *Neuropathol. Appl. Neurobiol.* **27**, 281–290.

Shumaker DK, Dechat T, Kohlmaier A, Adam SA, Bozovsky MR, Erdos MR, Eriksson M, Goldman AE, Khuon S, Collins FS, Jenuwein T, Goldman RD (2006) Mutant nuclear lamin A leads to progressive alterations of epigenetic control in premature aging. *Proc. Natl Acad. Sci. USA* **103**, 8703–8708.

Somech R, Shaklai S, Amariglio N, Rechavi G, Simon AJ (2005) Nuclear envelopathies – raising the nuclear veil. *Pediatr. Res.* **57**, 8–15.

Spann TP, Moir RD, Goldman AE, Stick R, Goldman RD (1997) Disruption of nuclear lamin organisation alters the distribution of replication factors and inhibits DNA synthesis. *J. Cell Biol.* **136**, 1201–1212.

Stehbens WE, Wakefield SJ, Gilbert-Barness E, Olson RE, Ackerman J (1999) Histological and ultrastructural features of atherosclerosis in progeria. *Cardiovasc. Pathol.* **8**, 29–39.

Stein GH, Dulic V (1998) Molecular mechanisms for the senescent cell cycle arrest. *J. Investig. Dermatol. Symp. Proc.* **3**, 14–18.

Stierle V, Couprie J, Ostlund C, Krimm I, Zinn-Justin S, Hossenlopp P, Worman HJ, Courvalin JC, Duband-Goulet I (2003) The carboxyl-terminal region common to lamins A and C contains a DNA binding domain. *Biochemistry* **42**, 4819–4828.

Sullivan T, Escalante-Alcalde D, Bhatt H, Anver M, Bhat N, Nagashima K, Stewart CL, Burke B (1999) Loss of A-type lamin expression compromises nuclear envelope integrity leading to muscular dystrophy. *J. Cell Biol.* **174**, 913–920.

Taniura H, Glass C, Gerace L (1995) A chromatin binding site in the tail domain of nuclear lamins that interacts with core histones. *J. Cell Biol.* **131**, 33–44.

Taylor MR, Slavov D, Gajewski A, Vlcek S, Ku L, Fain PR, Carniel E, Di Lenarda A, Sinagra G, Boucek MM, Cavanaugh J, Graw SL, Ruegg P, Feiger J, Zhu X, Ferguson DA, Bristow MR, Gotzmann J, Foisner R, Mestroni L; Familial Cardiomyopathy Registry Research Group (2005) Thymopoietin (lamina-associated polypeptide 2) gene mutation associated with dilated cardiomyopathy. *Hum. Mutat.* **26**, 566–574.

Thomas DM, Yang HS, Alexander K, Hinds PW (2003) Role of the retinoblastoma protein in differentiation and senescence. *Cancer Biol. Ther.* **2**, 124–130.

Tsukahara T, Tsujino S, Arahata K (2002) CDNA microarray analysis of gene expression in fibroblasts of patients with X-linked Emery-Dreifuss muscular dystrophy. *Muscle Nerve* **25**, 898–901.

Varela I, Cadinanos J, Pendas AM, Gutierrez-Fernandez A, Folgueras AR, Sanchez LM, Zhou Z, Rodriguez FJ, Stewart CL, Vega JA, Tryggvason K, Freije JM, Lopez-Otin C (2005) Accelerated ageing in mice deficient in Zmpste24 protease is linked to p53 signalling activation. *Nature* **437**, 564–568.

Verheijen R, Kuijpers HJ, Schlingemann RO, Boehmer AL, van Driel R, Brakenhoff GJ, Ramaekers FC (1989a) Ki-67 detects a nuclear matrix-associated proliferation-related antigen. I. Intracellular localization during interphase. *J. Cell Sci.* **92**, 123–130.

Verheijen R, Kuijpers HJ, van Driel R, Beck JL, van Dierendonck JH, Brakenhoff GJ, Ramaekers FC (1989b) Ki-67 detects a nuclear matrix-associated proliferation-related antigen. II. Localization in mitotic cells and association with chromosomes. *J. Cell Sci.* **92**, 531–540.

Vigouroux C, Capeau J (2005) A-type lamin-linked lipodystrophies. *Novartis. Found Symp.* **264**, 166–177.

Wilson KL (2000) The nuclear envelope, muscular dystrophy and gene expression. *Trends Cell Biol.* **10**, 152–129.

Wojda A, Witt M (2003) Manifestations of ageing at the cytogenetic level. *J. Appl. Genet.* **44**, 383–399.

Zastrow MS, Vlcek S, Wilson KL (2004) Proteins that bind A-type lamins: integrating isolated clues. *J. Cell Sci.* **117**, 979–987.

Supplementary material

Lamin A/C and emerin distribution in human dermal fibroblasts containing mutations in A-type lamin and emerin.

In the cell lines used in this study, either emerin or lamin A and C are affected. Both these proteins are found in the nuclear envelope and both have DNA binding capabilities. Thus, we analysed the distribution of these proteins and the position of chromosomes normally associated with the nuclear lamina (Boyle *et al.*, 2001).

The distributions of A-type lamins and emerin were analysed in the cell lines described in Table 1. After indirect immunofluorescence analysis with anti-lamin A/C and emerin antibodies, cells were classified by the staining patterns displayed in Figure S1. The categories are nuclear envelope (NE) rim only (Figure S1A,F), NE with internal foci (Figure S1B,G), internal foci only (Figure S1I), honeycomb pattern (Figure S1C,H),

homogenous staining throughout the nucleus (Figure S1D) or negative (Figure S1E,J). Figure S1K and L show the fractions of cells displaying each pattern. Unlike lymphoblastoid cells (see Meaburn *et al*., 2005) A-type lamin and emerin distributions appear fairly normal apart from in R298C-/-delK37y- and ED5364 which both have mutations in emerin, resulting in loss of emerin at the NE. Indeed, ED5364 cell line at the time of fixation for FISH contained only 13% of the emerin found in control cells and an absence lamin C, as determined by Western blot (data not shown). In a small subset of nuclei in E358K, R482L and R527H-/- cells an abnormal honeycomb-like staining pattern of emerin was observed (Figure S1H). A similar staining pattern was also observed for anti-lamin A/C in R298C-/-delk37y/-, E358K, R482L, R527H-/-, R527H+/-F and R527P but not in AG06297 (Figure S1C). This is not a novel finding, the interesting distribution of these NE proteins has been observed in cell lines from laminopathy patients and in heterozygous carriers and was not seen in control HDF 1HD (Vigouroux *et al*, 2001; Novelli *et al*., 2002; Capanni *et al*., 2003; Muchir *et al*., 2004).

The following supplementary material is available for this article:

Fig. S1. Indirect immunofluorescence of lamin A/C and emerin in laminopathy. Laminopathy HDFs stained for the presence of lamin A/C (green, A–E) or emerin (green, F–J) and counter stained with DAPI (blue). A and F display representative nuclei with nuclear envelope rim only staining, B and G display representative nuclei with rim staining with internal foci, C and H display representative nuclei with honeycomb staining pattern, D displays a nucleus with a homogenous lamin A/C staining pattern, whereas I displays a nucleus with internal foci of anti-emerin staining and E and J display nuclei negative for anti-lamin A/C staining and anti-emerin staining, respectively. The scale bar = 10 μm. The fraction of cells from each cell line displaying the individual staining patterns are shown by histograms in K and L for anti-lamin A/C and anti-emerin staining, respectively. Homogenous staining for lamin A/C was observed in <1% of cells and is not displayed in the graph (Figure S1K).

This material is available as part of the online article from: http://www.blackwell-synergy.com/doi/abs/10.1111/j.1474-9726.2007.00270.x

(This link will take you to the article abstract).

Please note: Blackwell Publishing are not responsible for the content or functionality of any supplementary materials supplied by the authors. Any queries (other than missing material) should be directed to the corresponding author for the article.